

Role of Tensor Interaction as Salvation of Cluster Structure in ^{44}Ti

Chikako Ishizuka

*Laboratory for Zero-Carbon Energy, Institute of Innovative Research,
Tokyo Institute of Technology, 2-12-1-N1-9, Ookayama, Meguro-ku, Tokyo, 152-8550, Japan*

Hiroki Takemoto

*Faculty of Pharmacy, Osaka Medical and Pharmaceutical University,
4-20-1, Nasahara, Takatsuki, Osaka, 569-1094, Japan*

Yohei Chiba

*Department of Physics, Osaka City University, Osaka 558-8585, Japan
Nambu Yoichiro Institute of Theoretical and Experimental Physics (NITEP),
Osaka City University, Osaka 558-8585, Japan and
Research Center for Nuclear Physics (RCNP), Osaka University, Ibaraki 567-0047, Japan*

Akira Ono

*Department of Physics, Graduate School of Science, Tohoku University,
6-3, Aramaki Aza-Aoba, Aoba-ku, Sendai 980-8578, Japan*

Naoyuki Itagaki

*Yukawa Institute for Theoretical Physics, Kyoto University,
Kitashirakawa Oiwake-Cho, Kyoto 606-8502, Japan*

(Dated: February 22, 2022)

Background: The ^{44}Ti nucleus has been known to have a $^{40}\text{Ca} + \alpha$ cluster structure, and inversion doublet structure has been observed; however, α cluster structure tends to be washed out when the breaking of the α cluster is allowed due to the spin-orbit interaction. Nevertheless, α clustering in medium-heavy nuclei is quite a hot subject recently.

Purpose: The tensor interaction has been known to play an essential role in the strong binding of the ^4He nucleus, which induces the two-particle-two-hole (2p2h) excitation. Since this excitation is blocked when another nucleus approaches, it is worthwhile to show whether the tensor effect works to keep the distance between ^4He and ^{40}Ca and becomes the salvation of the clustering in ^{44}Ti .

Methods: The spin-orbit effect is included in the cluster model by using the antisymmetrized quasi cluster model (AQCM) developed by the authors. We have also developed an improved version of the simplified method to include the tensor contribution (*i*SMT), which allows us to estimate the tensor effect within the cluster model. The competition of these two is investigated in the medium-heavy mass region for the first time.

Results: According to AQCM, the spin-orbit interaction completely breaks the α cluster and restores the symmetry of jj -coupling shell model when the α cluster approaches the ^{40}Ca core. On the other hand, *i*SMT gives a large distance between α and ^{40}Ca due to the tensor effect.

Conclusions: In ^{44}Ti , because of the strong spin-orbit and tensor contributions, two completely different configurations (jj -coupling shell model and cluster states) almost degenerate, and their mixing becomes important.

Owing to its distinctly large binding energy, ^4He becomes a good subsystem called an α cluster in the nuclear systems. Not only in the light-mass region, but also in the medium-heavy region, the α cluster structure has been investigated. From the theoretical side, the ^{44}Ti nucleus has been predicted to have a $^{40}\text{Ca} + \alpha$ cluster structure [1], and experimentally, the inversion doublet structure has been observed [2, 3], which supports the existence of cluster structure. The cluster structure of ^{44}Ti is also important in nuclear astrophysics; ^{44}Ti is one of the key elements for explosive nucleosynthesis in core-collapse supernovae and the $^{40}\text{Ca}(\alpha, \gamma)^{44}\text{Ti}$ reaction has been considered to be the main source for the production [4].

In a simple description with an α cluster wave function, the contribution of the non-central interactions (spin-

orbit and tensor interactions) vanishes owing to the spin and isospin saturation. It is, however, widely known that one of the non-central interactions, the spin-orbit interaction, is important in explaining the magic numbers of 28, 50, and 126 of the jj -coupling shell model [5]. If we allow the breaking of the α cluster(s), the cluster and shell structures compete with each other due to the spin-orbit interaction [6]. For instance, in ^{44}Ti , when we activate the degrees of freedom of four nucleons outside the ^{40}Ca core based on the antisymmetrized molecular dynamics (AMD), the α cluster structure is washed out due to the strong spin-orbit interaction, and they perform independent particle motions [7, 8]. A similar discussion was made also for ^{48}Ti , showing that the calculated reduced width amplitude of α cluster structure is the order of magnitude smaller than the one expected from the ex-

periment [9]. Therefore, how the α cluster structure survives in the medium-heavy region is quite an important subject, and many efforts have been devoted both from the theoretical and experimental sides [10, 11].

To quantitatively discuss the cluster-shell competition transparently, we have developed an antisymmetrized quasi cluster model (AQCM) [12–25], which enables us to smoothly transform α -cluster model wave functions to jj -coupling shell model ones even within a single Slater determinant. The spin-orbit effect is included by breaking α clusters with a control parameter Λ in this model, and such clusters that feel spin-orbit interaction are called quasi clusters. The cluster-shell competition can be described with the parameter Λ and the distance(s) between clusters.

The effect of another non-central interaction, the tensor interaction, is included by using a different model, i SMT also developed by us [26]. By applying i SMT to the four- α cluster structure of ^{16}O , the tensor interaction has been shown to increase the distances among α clusters. This is because the tensor interaction induces the 2p2h excitation of α cluster(s), but this is blocked when other α clusters approach, and the attractive tensor contribution is suppressed. As a result, the tensor interaction works to keep the relative distances between clusters. This i SMT was reformulated as high-momentum antisymmetrized molecular dynamics [27] AQCM-T [28, 29], and it has been possible to explain the mechanism of the α - α clustering in ^8Be starting with a realistic nucleon-nucleon interaction. An essential role is played by the tensor suppression effect at short relative distances.

In this study, we discuss the competition of the spin-orbit and tensor contributions in ^{44}Ti . The spin-orbit contribution is included by AQCM, which works to wash out the cluster structure. The tensor contribution is included by i SMT, which enhances the relative distance between clusters. The tensor interaction is found to be the salvation of the cluster structure.

Both in AQCM and i SMT, the single particle wave function has a Gaussian shape [30];

$$\phi_i = \left(\frac{2\nu}{\pi}\right)^{\frac{3}{4}} \exp\left[-\nu(\mathbf{r}_i - \boldsymbol{\zeta}_i)^2\right] \eta_i, \quad (1)$$

where η_i represents the spin-isospin part of the wave function, and $\boldsymbol{\zeta}_i$ is a parameter representing the center of a Gaussian wave function for the i -th particle. In the traditional cluster model (Brink model), the values $\boldsymbol{\zeta}_i = \mathbf{R}$ are common for four nucleons with different $\eta_i = \chi^{\tau,\sigma}$, which is the definition of the α cluster. We give different \mathbf{R} values for other cluster(s) if exists, and the ^{40}Ca core is constructed with ten α clusters with small (0.2 fm) relative distances. After the antisymmetrization, it becomes identical to the closed-shell configuration of the shell model. The size parameter ν is chosen to be 0.13 fm^{-2} , which gives the optimal energy (-339.51 MeV , with an interaction explained later) and a reasonable radius (root mean square (rms) matter radius of 3.38 fm) for ^{40}Ca . We add one α cluster outside the ^{40}Ca core in ^{44}Ti .

For the inclusion of the spin-orbit effect, we adopt AQCM. The four nucleons in the α cluster outside of the ^{40}Ca core is transformed into jj -coupling shell model based on the AQCM, by which the contribution of the spin-orbit interaction due to the breaking of α clusters is included. Here the $\boldsymbol{\zeta}_i$ values are changed to complex numbers. When the original value of the Gaussian center parameter $\boldsymbol{\zeta}_i$ is \mathbf{R} , which is real and related to the spatial position of this nucleon, it is transformed by adding the imaginary part as

$$\boldsymbol{\zeta}_i = \mathbf{R} + i\Lambda \mathbf{e}_i^{\text{spin}} \times \mathbf{R}, \quad (2)$$

where $\mathbf{e}_i^{\text{spin}}$ is a unit vector for the intrinsic-spin orientation of this nucleon. The control parameter Λ is associated with the breaking of the cluster, and two nucleons with opposite spin orientation have $\boldsymbol{\zeta}_i$ values that are complex conjugate to each other. This situation corresponds to the time-reversal motion of two nucleons. After this transformation, the α cluster is called a quasi cluster. The four nucleons are transformed to the $(f_{7/2})^4$ configuration of the jj -coupling shell model at the limit of $|\mathbf{R}| \rightarrow 0$ and $\Lambda = 1$, when the ^{40}Ca core is located at the origin.

For the inclusion of the rank-two non-central interaction, the tensor interaction, we adopt i SMT [26]. The tensor interaction has a feature that the second-order effect is much stronger than the first-order one; therefore 2p2h configurations are important. To incorporate such configurations in i SMT, the Gaussian center parameters for the four nucleons in ^4He (in the example that ^4He is located at \mathbf{R}) are shifted by adding the imaginary parts in the following way;

$$\begin{aligned} \boldsymbol{\zeta}_{p\uparrow} &= \mathbf{R} + i d \mathbf{e}_z, \\ \boldsymbol{\zeta}_{n\uparrow} &= \mathbf{R}, \\ \boldsymbol{\zeta}_{p\downarrow} &= \mathbf{R}, \\ \boldsymbol{\zeta}_{n\downarrow} &= \mathbf{R} - i d \mathbf{e}_z. \end{aligned} \quad (3)$$

Here, the Gaussian center parameters of proton spin-up ($\boldsymbol{\zeta}_{p\uparrow}$) and neutron spin-down ($\boldsymbol{\zeta}_{n\downarrow}$) are shifted, with the parameter d taken to be 1.5, 3.0, \dots 15.0 fm (10 Slater determinants in addition to $d = 0$ fm). The spin orientation is quantized along the z -axis, and \mathbf{e}_z is a unit vector for this axis. We also prepare the basis states, where neutron spin-up ($\boldsymbol{\zeta}_{n\uparrow}$) is shifted in stead of neutron spin-down;

$$\begin{aligned} \boldsymbol{\zeta}_{p\uparrow} &= \mathbf{R} + i d \mathbf{e}_z, \\ \boldsymbol{\zeta}_{n\uparrow} &= \mathbf{R} - i d \mathbf{e}_z, \\ \boldsymbol{\zeta}_{p\downarrow} &= \mathbf{R}, \\ \boldsymbol{\zeta}_{n\downarrow} &= \mathbf{R}. \end{aligned} \quad (4)$$

Eventually, we superpose these 21 Slater determinants in total based on the generator coordinate method (GCM), and coefficients for the linear combination are determined by diagonalizing the norm and Hamiltonian matrices.

In the original version, SMT, the real part was shifted to describe them; however, the effect has been quite insufficient [31]. On the other hand, in the improved version of SMT (i SMT) explained above, the imaginary part

of the Gaussian center parameters is shifted instead of the real part. This is much suited for describing the high-momentum components since the imaginary part of Gaussian center parameter directly corresponds to the nucleon momentum.

The Hamiltonian (\hat{H}) consists of kinetic energy (\hat{T}) and potential energy (\hat{V}) terms,

$$\hat{H} = \hat{T} + \hat{V}, \quad (5)$$

and the kinetic energy term is described as one-body operator,

$$\hat{T} = \sum_i \hat{t}_i - T_{\text{cm}}, \quad (6)$$

and the center of mass kinetic energy (T_{cm}), which is constant, is subtracted. The potential energy has central (\hat{V}_{central}), spin-orbit ($\hat{V}_{\text{spin-orbit}}$), tensor (\hat{V}_{tensor}), and the Coulomb parts.

For the central part of the nucleon-nucleon interaction (\hat{V}_{central}), in many conventional cluster studies, the Volkov interaction [32] has been often used as the effective nucleon-nucleon interaction. Although this interaction is capable of describing various properties of light nuclei, it consists of only two ranges and is not designed to well describe the medium-heavy region. In the present case, if we adjust the Majorana exchange parameter to reproduce the binding energy of ^{40}Ca , it gives for ^{44}Ti a too deep binding between ^4He and ^{40}Ca with a very small distance between them, which is not consistent with a well-developed cluster structure, even before taking into account the breaking of the α cluster. On the other hand, if we change the Majorana parameter to adjust the binding energy of ^{44}Ti from the $^{40}\text{Ca} + ^4\text{He}$ threshold energy, the $^{40}\text{Ca} + ^4\text{He}$ cluster structure does appear (if we do not include the breaking of the α cluster), but then the internal energy of ^{40}Ca becomes very underbinding. The internal binding energy of ^{40}Ca is indeed not explicitly needed in the actual calculation, but the obtained results are unreliable if this value is quite different from the experimental value. Therefore, we need to adopt an alternative nucleon-nucleon interaction suitable for describing the medium-heavy nuclei. Here we introduce the one developed by one of the authors (H.T.), which has three ranges;

$$\hat{V}_{\text{central}} = \frac{1}{2} \sum_{i \neq j} \sum_{\alpha=1}^3 V_{\alpha} \exp[-(\mathbf{r}_i - \mathbf{r}_j)^2 / \mu_{\alpha}^2] (W_{\alpha} + M_{\alpha} P^r)_{ij}. \quad (7)$$

Here, $P^r = -P^{\sigma} P^{\tau}$ represents the exchange of spatial part of the wave functions of interacting two nucleons, and $W_{\alpha} = 1 - M_{\alpha}$, where M_{α} is Majorana exchange parameter. The parameters are listed in Table I. This interaction is designed to reproduce the properties in a wide mass-number range. For instance, for the symmetric nuclear matter, the interaction gives the saturation point at the binding energy $E/A = -15.6$ MeV and the

TABLE I. The parameter set for the central part of the nucleon-nucleon interaction (\hat{V}_{central}) adopted in the calculation (Eq. 7) developed by one of the authors (H.T.).

α	V_{α} (MeV)	μ_{α} (fm)	M_{α}
1	611.88	0.81	-0.06979
2	-287.21	1.62	0.55326
3	57.972	2.43	0.68020

Fermi momentum $k_F = 1.29 \text{ fm}^{-1}$. Also, it gives the incompressibility of $K = 239$ MeV.

For the spin-orbit part ($\hat{V}_{\text{spin-orbit}}$), Gaussian three-range soft-core (G3RS) interaction [33], which is a realistic interaction originally determined to reproduce the nucleon-nucleon scattering phase shift, is adopted;

$$\hat{V}_{\text{spin-orbit}} = \frac{1}{2} \sum_{i \neq j} V_{ij}^{ls}, \quad (8)$$

$$V_{ij}^{ls} = V_{ls} (e^{-d_1(\mathbf{r}_i - \mathbf{r}_j)^2} - e^{-d_2(\mathbf{r}_i - \mathbf{r}_j)^2}) P(^3O) \mathbf{L} \cdot \mathbf{S}. \quad (9)$$

For the strength, $V_{ls} = 1600\text{--}2000$ MeV has been suggested to reproduce the scattering phase shift of ^4He and n [34]. We adopt $V_{ls} = 1800$ MeV, which reproduces various properties of ^{12}C [20, 25]. There has been discussion that the tensor contribution is included in this scattering phase shift [35, 36], and thus this strength can be considered as the maximum value.

For the tensor part (V_{tensor}), we use Furutani interaction [37]. This interaction nicely reproduces the tail region of the one-pion-exchange potential.

The energy curves for the 0^+ state of ^{44}Ti are shown in Fig. 1 as a function of the distance between quasi cluster (^4He) and ^{40}Ca . The dotted curve is for the $\alpha + ^{40}\text{Ca}$ cluster model (Brink model, $\Lambda = 0$) and the solid curve is the result of AQCM, where the optimal Λ value is adopted for each distance. The horizontal dotted line at -339.51 MeV noted as $^{40}\text{Ca} + 4N$ (Th.) shows the theoretical $^{40}\text{Ca} + 4N$ threshold energy. Experimentally, the ^{40}Ca nucleus has the energy of -342.52 MeV noted as $^{40}\text{Ca} + 4N$ (Exp.) and ^{44}Ti is bound from this threshold by 32.95 MeV. There is no spin-orbit contribution for the dotted curve (Brink model), which has the energy minimum around the relative distance of ~ 4 fm, and the binding energy there is much less than the experimental value (32.95 MeV below the threshold). On the other hand, in the solid curve, AQCM, the α cluster can be broken by introducing the Λ parameter, which is variationally determined, and the spin-orbit contribution is properly included. This effect is especially large at the short distances between ^{40}Ca and ^4He . The binding becomes deeper than the dotted curve (Brink model) with decreasing the relative distance, where the binding energy approaches the experimental value. This means that the α cluster structure is significantly destroyed by the spin-orbit interaction when we allow the breaking of

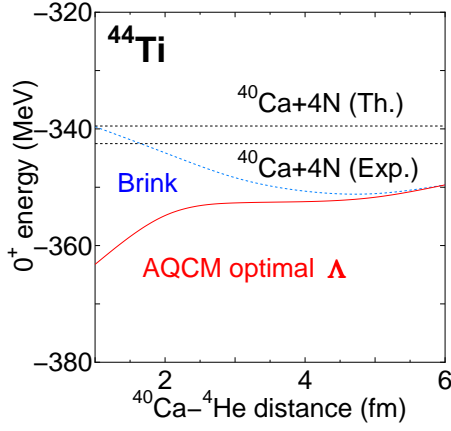


FIG. 1. Energy curves for the 0^+ state of ^{44}Ti as a function of the distance between ^4He and ^{40}Ca . The dotted curve is for the $\alpha + ^{40}\text{Ca}$ cluster model (Brink model) and the solid curve is the result of AQCM, where the optimal Λ value is adopted for each distance.

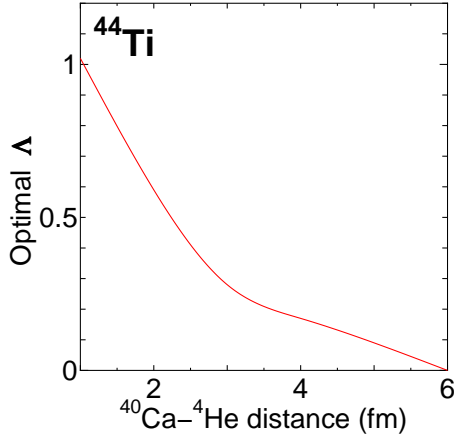


FIG. 2. Optimal Λ value of AQCM introduced to the ^4He cluster outside of the ^{40}Ca core for the 0^+ state of ^{44}Ti as a function of the distance between quasi cluster (^4He) and ^{40}Ca .

the α cluster, and thus the result indicates that the jj -coupling shell model state may be realized in the ground state of ^{44}Ti .

This possibility is confirmed by the optimal Λ value of AQCM, which is introduced for the ^4He cluster outside of the ^{40}Ca core. The adopted Λ value for the 0^+ state of ^{44}Ti is shown in Fig. 2 as a function of the distance between ^4He and ^{40}Ca . The value becomes almost unity at small relative distances, and α cluster structure is found to be completely washed out, and the four nucleons are changed into independent particles with the $(f_{7/2})^4$ configuration of the jj -coupling shell model. On the other hand, when the relative distance increases, the Λ value decreases and the difference between the α cluster model and AQCM becomes small.

The calculated rms matter radius for the 0^+ state of

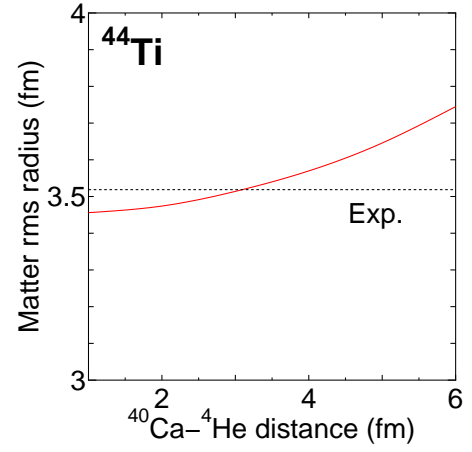


FIG. 3. Calculated rms matter radius for the 0^+ state of ^{44}Ti as a function of the distance between ^4He and ^{40}Ca . The optimal Λ value of AQCM is adopted for each distance.

^{44}Ti is shown in Fig. 3 as a function of the relative distance between ^4He and ^{40}Ca . The optimal Λ value of AQCM is adopted for each distance. Experimentally, the rms charge radii of ^{40}Ca and ^{44}Ti are 3.4776(19) fm and 3.6115(51) fm, respectively. The difference is 0.134 fm. In our model, the rms matter radius of ^{40}Ca is 3.38 fm, which is quite consistent with the experimental charge radius. Here we face one problem; to explain this increase of the rms radius from ^{40}Ca to ^{44}Ti (experimentally 0.134 fm), the distance between ^4He and ^{40}Ca must have a certain value. According to AQCM, the lowest energy of ^{44}Ti is obtained at the relative distance of 1 fm and α cluster structure vanishes, but this relative distance of 1 fm gives a small rms radius. The figure tells us that we need ~ 3 fm as the distance between the two clusters to explain the observed increase of the rms radius from ^{40}Ca to ^{44}Ti . This means that the cluster structure must survive to some extent in the ground state of ^{44}Ti . The experimental matter radius of ^{44}Ti can be deduced as 3.519 fm from the measured charge radius, which is shown by the dotted line, and it crosses with the calculated result (solid line) around the intercluster distance of 3 fm.

Therefore, as the next step, we investigate the possibility of the tensor effect as the salvation of the cluster structure. We introduce $i\text{SMT}$ and include the tensor effect. The energy of the 0^+ state of ^{44}Ti is shown in Fig. 4 as a function of the distance between ^4He and ^{40}Ca . Here again, the horizontal dotted lines noted as $^{40}\text{Ca} + 4N$ (Th.) and $^{40}\text{Ca} + 4N$ (Exp.) represent the theoretical and experimental $^{40}\text{Ca} + 4N$ threshold energies, respectively. The solid curve is the result of $i\text{SMT}$, and again, the dotted curve is for the $\alpha + ^{40}\text{Ca}$ cluster model (Brink model). The tensor effect becomes almost zero at the limit of a small distance between the two clusters (tensor suppression effect), but α cluster model and $i\text{SMT}$ give quite different results at large relative distances. This means that the tensor suppression effect disappears at

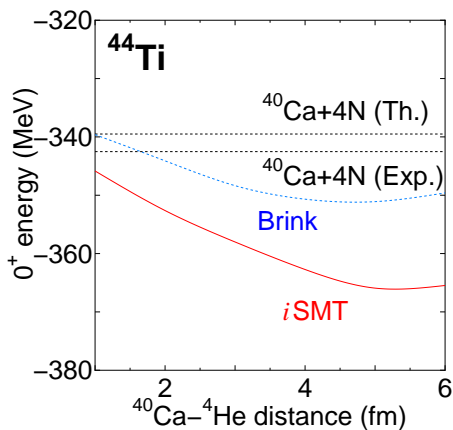


FIG. 4. Energy of the 0^+ state of ^{44}Ti as a function of the distance between ^4He and ^{40}Ca . The dotted curve is for the $\alpha+^{40}\text{Ca}$ cluster model (Brink model) and the solid curve is the result of $i\text{SMT}$.

large relative distances. The minimum energy of $i\text{SMT}$ is given around the relative distance of 5 fm. It can be confirmed that the tensor interaction induces the clustering of the system. Here, the minimum energy in $i\text{SMT}$ is almost the same as in AQCM, which was discussed previously. Therefore, in the ground state of ^{44}Ti , it is considered that completely different structures of the jj -coupling shell model (AQCM) and $^4\text{He} + ^{40}\text{Ca}$ clustering ($i\text{SMT}$) degenerate. If we mix two configurations with equal weight, the experimentally observed difference of radii between ^{40}Ca and ^{44}Ti could be reproduced.

Finally, we couple AQCM and $i\text{SMT}$. The AQCM is represented by the basis state with the $^{40}\text{Ca}-^4\text{He}$ distance of 1 fm with the optimal Λ , while $i\text{SMT}$ is by the distance of 5 fm. They have the 0^+ energies of -362.2 MeV and -365.5 MeV, and the calculated rms matter radii are 3.46 fm and 3.63 fm. After coupling these states, two 0^+ states are obtained at -366.2 MeV and -362.9 MeV. The coefficients for the linear combination of 21 basis states for $i\text{SMT}$ are newly determined after coupling with the AQCM basis state; thus it is not a numerical error that the higher state before the coupling (AQCM) is not pushed up in energy after the diagonalization of the Hamiltonian matrix. The rms matter radius of the lowest state is 3.61 fm, and the increase from the ^{40}Ca one of 0.23 fm is overestimated compared to the experimental one (0.134 fm). Experimentally, the second 0^+ state is observed at $E_x = 1.90$ MeV. The present level spacing of 3.3 MeV for the two 0^+ states is larger than this value. These results would suggest that cluster configuration mixes slightly stronger than reality, and thus we have to

perform more detailed investigations. For instance, the central interaction should be reconsidered after switching on the tensor interaction. In addition, the basis states of AQCM with the relative intercluster distance less than 1 fm should be included, and more states with different intercluster distances should be superposed. Also, the double projection has to be performed during the angular momentum projection process. These effects are expected to reproduce more precisely the ground state energy compared to the experiment.

In this article, the α cluster structure in the ^{44}Ti nucleus was investigated, in the viewpoint of the cluster-shell competition. The ^{44}Ti nucleus has been known to have a $^{40}\text{Ca}+\alpha$ cluster structure and inversion doublet structure has been observed; however, α cluster structure is washed out when we allow the breaking of the cluster and switch on the spin-orbit interaction. Here, we focused on the role of the tensor interaction as the salvation of the cluster structure, which has been known to play an essential role in the strong binding of the ^4He nucleus; the strong tensor effect favors the large distance between the clusters. Although the traditional α cluster models cannot take into account the non-central interaction, we developed AQCM and $i\text{SMT}$ to include the spin-orbit and tensor contributions in the cluster model, respectively. Here, the two models predicted different ground states almost at the same energy. Therefore, in the true ground state of ^{44}Ti , completely different structures of the jj -coupling shell model (AQCM) and $^4\text{He} + ^{40}\text{Ca}$ clustering ($i\text{SMT}$) are considered to mix. After coupling AQCM and $i\text{SMT}$, two 0^+ states are obtained at -366.2 MeV and -362.9 MeV. The present level spacing of 3.3 MeV is slightly larger than the experimental value ($E_x = 1.90$ MeV), which requires further detailed investigations.

In the present study, we just added the tensor interaction in the Hamiltonian; however, in this case, the central interaction should be reconsidered. Also, only the angular momentum projection of the total system was performed in the present study, but the double projection of subsystem (^4He) and total system is expected to contribute to the lowering of the cluster states. These effects will be examined in the forthcoming work.

Nevertheless, it is intriguing to point out that the tensor interaction works as the salvation of the cluster structure that could be otherwise destroyed by the spin-orbit interaction.

ACKNOWLEDGMENTS

Numerical calculations have been performed at Yukawa Institute for Theoretical Physics, Kyoto University (Yukawa-21).

[1] F. Michel, G. Reidemeister, and S. Ohkubo, Evidence for alpha-particle clustering in the ^{44}Ti nucleus, *Phys. Rev. Lett.* **57**, 1215 (1986).

- [2] T. Yamaya, S. Oh-ami, M. Fujiwara, T. Itahashi, K. Katori, M. Tosaki, S. Kato, S. Hatori, and S. Ohkubo, Existence of α -cluster structure in ^{44}Ti via the $(^6\text{Li}, d)$ reaction, *Phys. Rev. C* **42**, 1935 (1990).
- [3] T. Yamaya, K. Katori, M. Fujiwara, S. Kato, and S. Ohkubo, Alpha-Cluster Study of ^{40}Ca and ^{44}Ti by the $(^6\text{Li}, d)$ Reaction, *Progress of Theoretical Physics Supplement* **132**, 73 (1998), <https://academic.oup.com/ptps/article-pdf/doi/10.1143/PTP.132.73/5328434/132-73.pdf>.
- [4] H. Nassar, M. Paul, I. Ahmad, Y. Ben-Dov, J. Caggiano, S. Ghelberg, S. Goriely, J. P. Greene, M. Hass, A. Heger, A. Heinz, D. J. Henderson, R. V. F. Janssens, C. L. Jiang, Y. Kashiv, B. S. Nara Singh, A. Ofan, R. C. Pardo, T. Pennington, K. E. Rehm, G. Savard, R. Scott, and R. Vondrasek, $^{40}\text{Ca}(\alpha, \gamma)^{44}\text{Ti}$ reaction in the energy regime of supernova nucleosynthesis, *Phys. Rev. Lett.* **96**, 041102 (2006).
- [5] M. G. Mayer and H. G. Jensen, “Elementary theory of nuclear shell structure”, John Wiley, Sons, New York, Chapman, Hall, London (1955).
- [6] N. Itagaki, S. Aoyama, S. Okabe, and K. Ikeda, Cluster-shell competition in light nuclei, *Phys. Rev. C* **70**, 054307 (2004).
- [7] M. Kimura and H. Horiuchi, Coexistence of cluster structure and superdeformation in ^{44}Ti , *Nuclear Physics A* **767**, 58 (2006).
- [8] Y. Chiba, M. Kimura, and Y. Taniguchi, Isoscalar dipole transition as a probe for asymmetric clustering, *Phys. Rev. C* **93**, 034319 (2016).
- [9] Y. Taniguchi, K. Yoshida, Y. Chiba, Y. Kanada-En’yo, M. Kimura, and K. Ogata, Unexpectedly enhanced α -particle preformation in ^{48}Ti probed by the $(p, p\alpha)$ reaction, *Phys. Rev. C* **103**, L031305 (2021).
- [10] S. Typel, G. Röpke, T. Klähn, D. Blaschke, and H. H. Wolter, Composition and thermodynamics of nuclear matter with light clusters, *Phys. Rev. C* **81**, 015803 (2010).
- [11] J. Tanaka, Z. Yang, S. Typel, S. Adachi, S. Bai, P. van Beek, D. Beaumel, Y. Fujikawa, J. Han, S. Heil, S. Huang, A. Inoue, Y. Jiang, M. Knösel, N. Kobayashi, Y. Kubota, W. Liu, J. Lou, Y. Maeda, Y. Matsuda, K. Miki, S. Nakamura, K. Ogata, V. Panin, H. Scheit, F. Schindler, P. Schrock, D. Symochko, A. Tamii, T. Uesaka, V. Wagner, K. Yoshida, J. Zenihiro, and T. Aumann, Formation of ^3He clusters in dilute neutron-rich matter, *Science* **371**, 260 (2021), <https://www.science.org/doi/pdf/10.1126/science.abe4688>.
- [12] N. Itagaki, H. Masui, M. Ito, and S. Aoyama, Simplified modeling of cluster-shell competition, *Phys. Rev. C* **71**, 064307 (2005).
- [13] H. Masui and N. Itagaki, Simplified modeling of cluster-shell competition in carbon isotopes, *Phys. Rev. C* **75**, 054309 (2007).
- [14] T. Yoshida, N. Itagaki, and T. Otsuka, Appearance of cluster states in ^{13}C , *Phys. Rev. C* **79**, 034308 (2009).
- [15] N. Itagaki, J. Cseh, and M. Płoszajczak, Simplified modeling of cluster-shell competition in ^{20}Ne and ^{24}Mg , *Phys. Rev. C* **83**, 014302 (2011).
- [16] T. Suhara, N. Itagaki, J. Cseh, and M. Płoszajczak, Novel and simple description for a smooth transition from α -cluster wave functions to jj -coupling shell model wave functions, *Phys. Rev. C* **87**, 054334 (2013).
- [17] N. Itagaki, H. Matsuno, and T. Suhara, General trans-formation of α cluster model wave function to jj -coupling shell model in various $4n$ nuclei, *Prog. Theor. Exp. Phys.* **2016**, 093D01 (2016).
- [18] H. Matsuno, N. Itagaki, T. Ichikawa, Y. Yoshida, and Y. Kanada-En’yo, Effect of $^{12}\text{C} + \alpha$ clustering on the $e0$ transition in ^{16}O , *Prog. Theor. Exp. Phys.* **2017**, 063D01 (2017).
- [19] H. Matsuno and N. Itagaki, Effects of cluster-shell competition and bcs-like pairing in ^{12}C , *Prog. Theor. Exp. Phys.* **2017**, 123D05 (2017).
- [20] N. Itagaki, Consistent description of ^{12}C and ^{16}O using a finite-range three-body interaction, *Phys. Rev. C* **94**, 064324 (2016).
- [21] N. Itagaki and A. Tohsaki, Nontrivial origin for the large nuclear radii of dripline oxygen isotopes, *Phys. Rev. C* **97**, 014307 (2018).
- [22] N. Itagaki, H. Matsuno, and A. Tohsaki, Explicit inclusion of the spin-orbit contribution in the tohsaki-horiuchi-schuck-röpke wave function, *Phys. Rev. C* **98**, 044306 (2018).
- [23] N. Itagaki, A. V. Afanasjev, and D. Ray, Possibility of ^{14}C cluster as a building block of medium-mass nuclei, *Phys. Rev. C* **101**, 034304 (2020).
- [24] N. Itagaki, T. Fukui, J. Tanaka, and Y. Kikuchi, ^8He and ^9Li cluster structures in light nuclei, *Phys. Rev. C* **102**, 024332 (2020).
- [25] N. Itagaki and T. Naito, Consistent description for cluster dynamics and single-particle correlation, *Phys. Rev. C* **103**, 044303 (2021).
- [26] N. Itagaki and A. Tohsaki, Improved version of a simplified method for including tensor effects in cluster models, *Phys. Rev. C* **97**, 014304 (2018).
- [27] T. Myo, H. Toki, K. Ikeda, H. Horiuchi, T. Suhara, M. Lyu, M. Isaka, and T. Yamada, High-momentum antisymmetrized molecular dynamics compared with tensor-optimized shell model for strong tensor correlation, *Progress of Theoretical and Experimental Physics* **2017**, 10.1093/ptep/ptx143 (2017), 111D01, <https://academic.oup.com/ptep/article-pdf/2017/11/111D01/21611281/ptx143.pdf>.
- [28] H. Matsuno, Y. Kanada-En’yo, and N. Itagaki, Tensor correlations in ^4He and ^8Be within an antisymmetrized quasicluster model, *Phys. Rev. C* **98**, 054306 (2018).
- [29] N. Itagaki, H. Matsuno, and Y. Kanada-En’yo, Short-range and tensor correlations in ^4He and ^8Be studied with the antisymmetrized quasi-cluster model, *Prog. Theor. Exp. Phys.* **2019**, 10.1093/ptep/ptz046 (2019), 063D02.
- [30] D. M. Brink, The alpha-particle model of light nuclei, *Proc. Int. School Phys. “Enrico Fermi”* **XXXVI**, 247 (1966).
- [31] N. Itagaki, H. Masui, M. Ito, S. Aoyama, and K. Ikeda, Simplified method to include the tensor contribution in α -cluster model, *Phys. Rev. C* **73**, 034310 (2006).
- [32] A. Volkov, Equilibrium deformation calculations of the ground state energies of $1p$ shell nuclei, *Nucl. Phys.* **74**, 33 (1965).
- [33] R. Tamagaki, Potential models of nuclear forces at small distances, *Prog. Theor. Phys.* **39**, 91 (1968).
- [34] S. Okabe, Y. Abe, and H. Tanaka, The structure of 9be nucleus by a molecular model, *Prog. Theor. Phys.* **57**, 866 (1977).
- [35] A. Arima and T. Terasawa, Spin-Orbit Splitting and Tensor Force. II, *Progress of Theoretical Physics* **23**, 115 (1960),

- <https://academic.oup.com/ptp/article-pdf/23/1/115/5439049/23-1-115.pdf>.
- [36] T. Myo, K. Katō, and K. Ikeda, Tensor Correlation in ^4He and Its Effect on the Doublet Splitting in ^5He , *Progress of Theoretical Physics* **113**, 763 (2005), <https://academic.oup.com/ptp/article-pdf/113/4/763/5123578/113-4-763.pdf>.
- [37] H. Furutani, H. Horiuchi, and R. Tamagaki, Structure of the Second 0^+ State of ^4He , *Progress of Theoretical Physics* **60**, 307 (1978), <https://academic.oup.com/ptp/article-pdf/60/1/307/5214924/60-1-307.pdf>.